Science Advances
AAAS

Supplementary Materials for

Geological processes mediate a microbial dispersal loop in the deep biosphere

Daniel A. Gittins *et al.*

Corresponding author: Daniel A. Gittins, daniel.gittins@ucalgary.ca

Sci. Adv. **8**, eabn3485 (2022)
DOI: 10.1126/sciadv.abn3485

The PDF file includes:

Other Supplementary Material for this manuscript includes the following:

Other Supplementary Materials for this manuscript include the following:

Movie S1. Seabed hydrocarbon seepage.

Table S1. Marine sediment core site locations and sample descriptions.

Table S2. Hydrocarbon geochemical measurements on marine sediment cores.

Table S3. ASV table with taxonomic classification of 16S rRNA gene amplicon libraries.

Table S4. Analysis of similarity (ANOSIM) test results.

Table S5. IndicSpecies Stat values.

Table S6. Taxonomic assignment.

Table S7. Metagenome-assembled genomes (MAGs).

Table S8. Summary of genes detected in metagenome-assembled genomes (MAGs).

Table S9. Sporulation genes annotated against Pfam, TIGRFAM and Swiss-Prot databases.

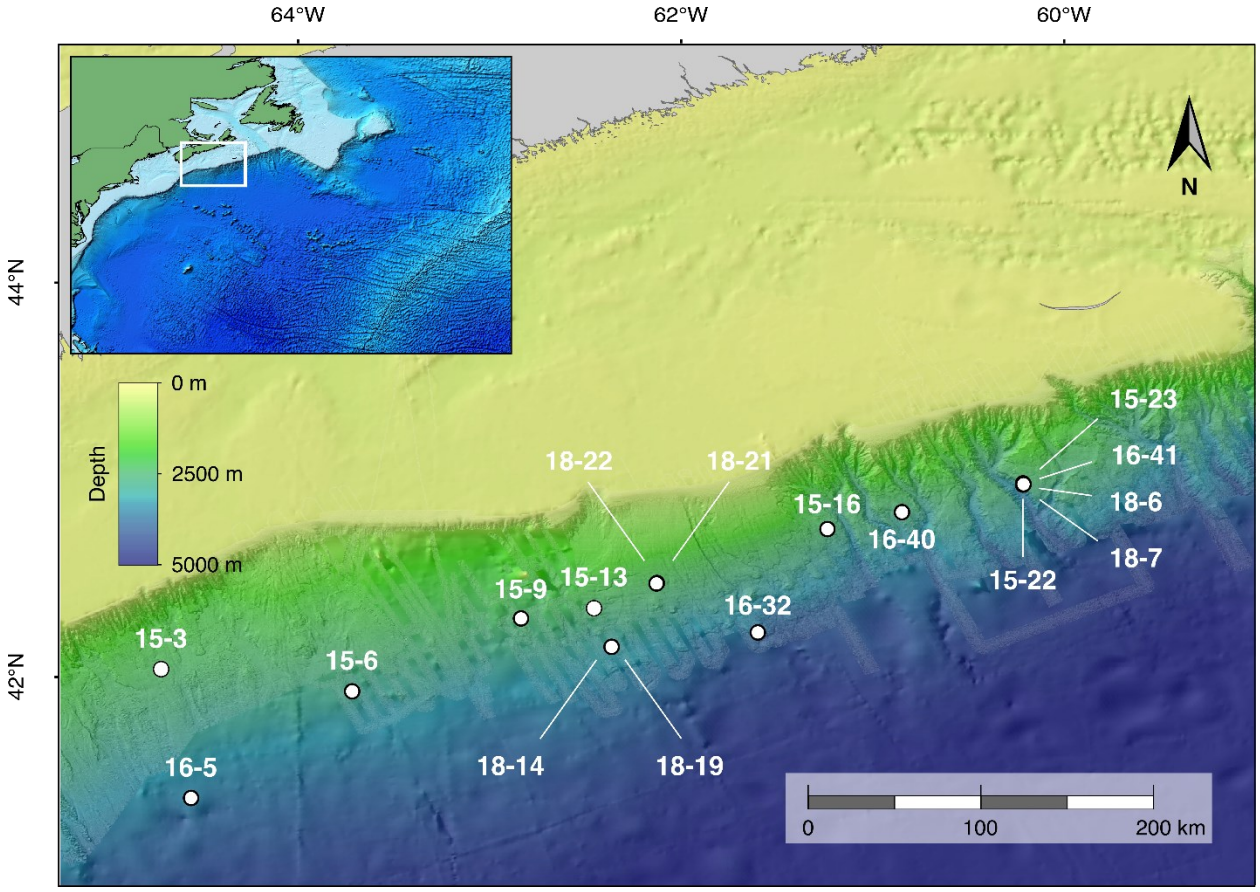

Fig. S1. Deep sea study sites in the NW Atlantic Ocean. Sediment coring locations on the Scotian Slope. The inset shows the extent of the 20,000 km^2 study area, approximately 200 km off the east coast of Nova Scotia, Canada, and 2,200 km west of the mid-Atlantic ridge (inset). Bathymetric map from the General Bathymetric Chart of the Oceans (GEBCO, www.gebco.net) and National Oceanic and Atmospheric Administration (NOAA, www.ngdc.noaa.gov/).

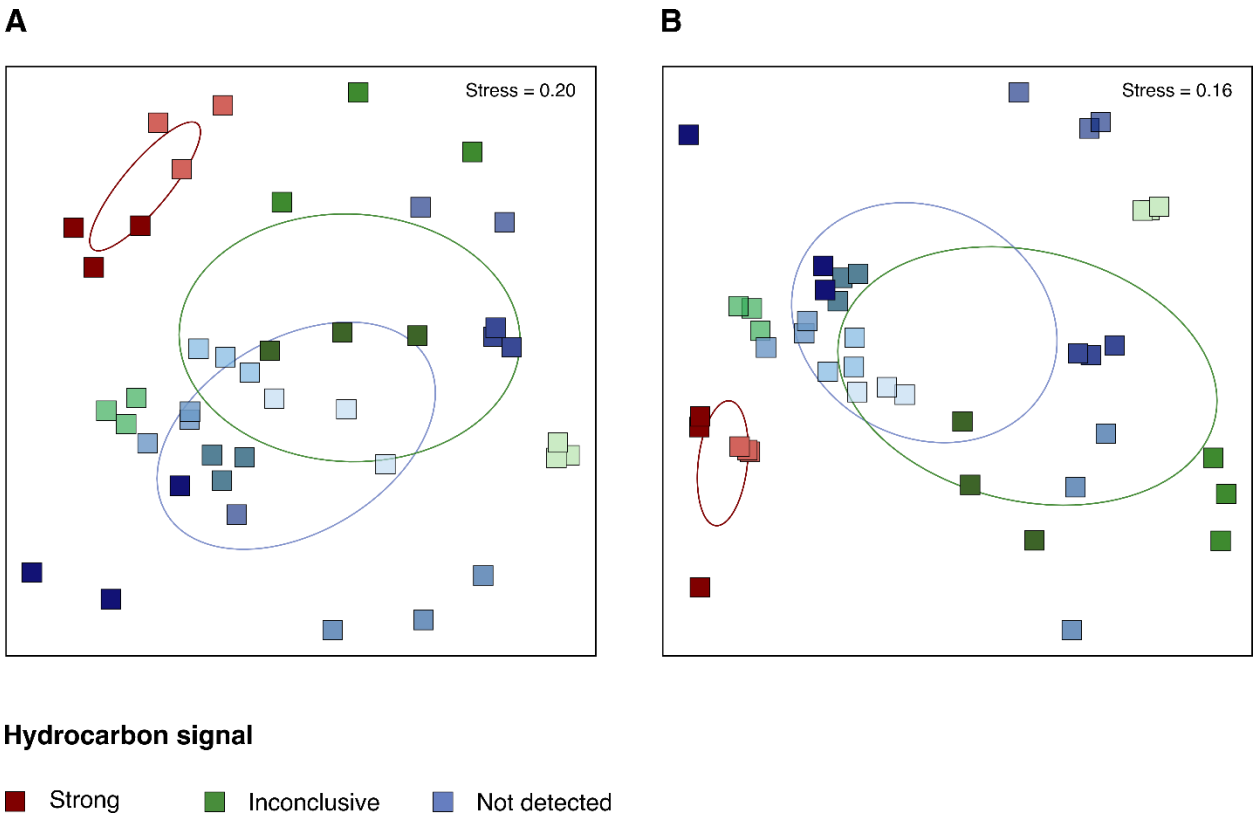

Fig. S2. Microbial community variance between core sites. Non-metric multidimensional scaling of the Bray-Curtis dissimilarity of the microbial community composition after sediment incubation at (**A**) 40°C and (**B**) 60°C (for 50°C incubations, see Fig. 2B). Red symbols indicate sites with strong geochemical evidence of hydrocarbons (*n*=2), green symbols indicate sites with inconclusive hydrocarbon signals (*n*=4), and blue symbols indicate sites where hydrocarbons were not detected (*n*=8). Triplicate amplicon libraries are plotted for each condition. Sites with strong thermogenic hydrocarbon signals have distinct microbial populations after high temperature incubation (see also table S4), relative to the sites without thermogenic hydrocarbon signals. This is indicated by standard deviation ellipses of the hydrocarbon groups.

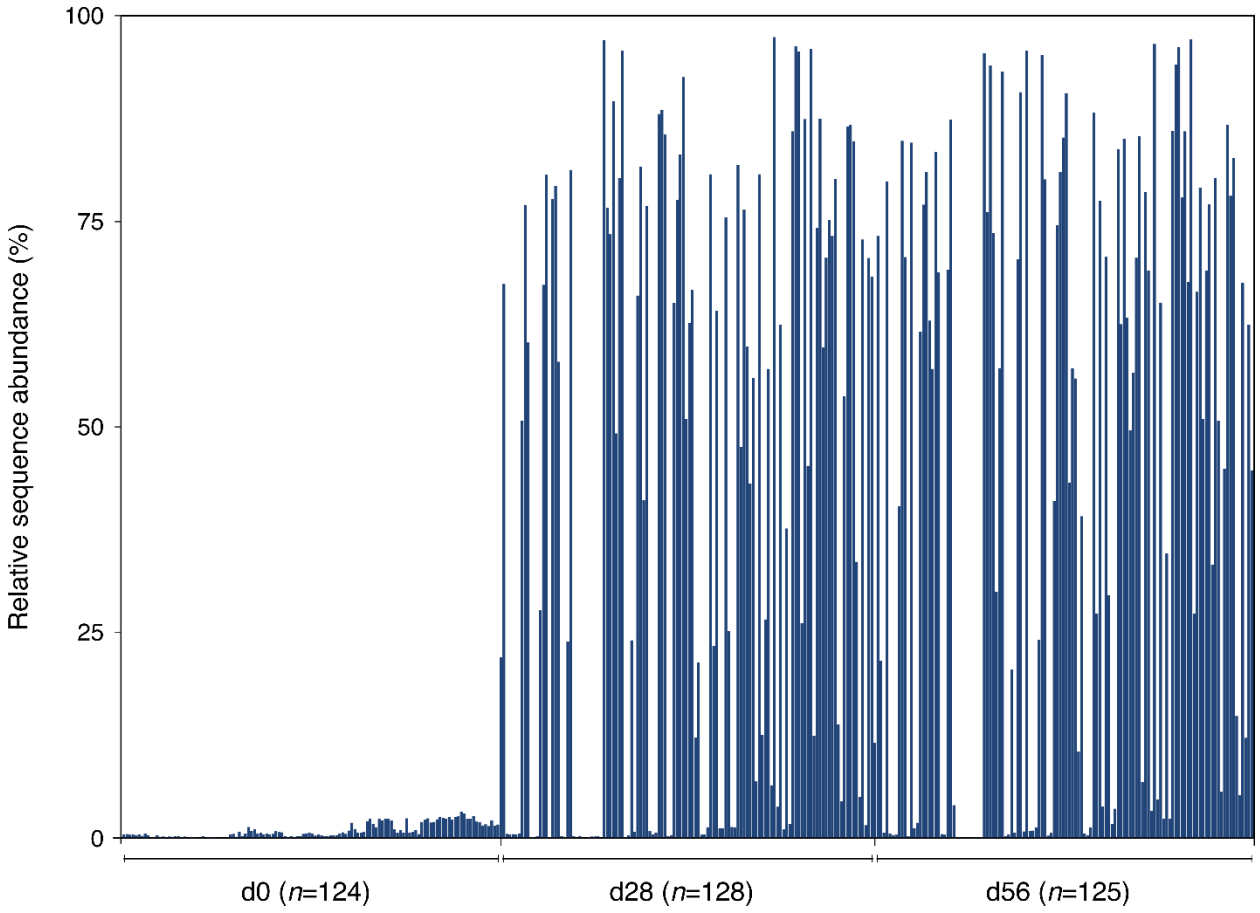

Fig. S3. Endospore germination and enrichment after high temperature incubation. Relative sequence abundance of *Firmicutes* in 372 libraries of 16S rRNA gene amplicons before (d0; post-pasteurisation) and after 28 and 56 days of anoxic incubation at 40, 50, or 60°C (see table S3 for detailed microbial community compositions). Each blue bar represents a single library of 4,635 subsampled reads, and demonstrates an increased proportion of *Firmicutes* following 28 and 56 days of incubation. The proportion of *Firmicutes* in d0 libraries was on average 0.9%, and was even lower in libraries from unpasteurized surface sediments, which are dominated by cold-adapted populations able to colonize seabed environments including hydrocarbon seeps (*23*).

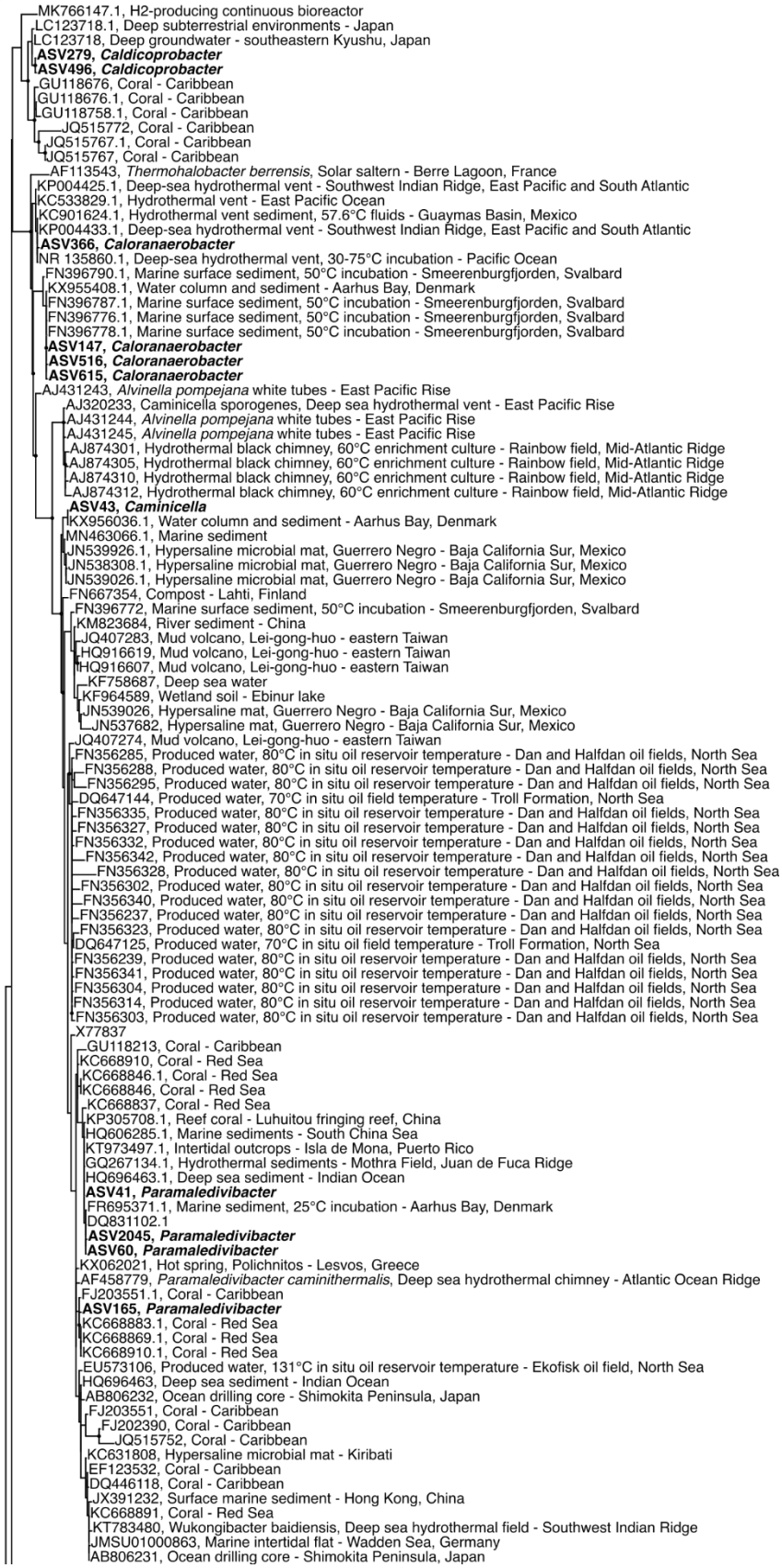
MK766147.1, H2-producing continuous bioreactor
LC123718.1, Deep subterrestrial environments - Japan
LC123718, Deep groundwater - southeastern Kyushu, Japan
ASV279, *Caldicoprobacter*
ASV496, *Caldicoprobacter*
GU118676, Coral - Caribbean
GU118676.1, Coral - Caribbean
GU118758.1, Coral - Caribbean
JQ515772, Coral - Caribbean
JQ515767.1, Coral - Caribbean
JQ515767, Coral - Caribbean
AF113543, *Thermohalobacter berrensis*, Solar saltern - Berre Lagoon, France
KP004425.1, Deep-sea hydrothermal vent - Southwest Indian Ridge, East Pacific and South Atlantic
KC533829.1, Hydrothermal vent - East Pacific Ocean
KC901624.1, Hydrothermal vent sediment, 57.6°C fluids - Guaymas Basin, Mexico
KP004433.1, Deep-sea hydrothermal vent - Southwest Indian Ridge, East Pacific and South Atlantic
ASV366, *Caloranaerobacter*
NR 135860.1, Deep-sea hydrothermal vent, 30-75°C incubation - Pacific Ocean
FN396790.1, Marine surface sediment, 50°C incubation - Smeerenburgfjorden, Svalbard
KX955408.1, Water column and sediment - Aarhus Bay, Denmark
FN396787.1, Marine surface sediment, 50°C incubation - Smeerenburgfjorden, Svalbard
FN396776.1, Marine surface sediment, 50°C incubation - Smeerenburgfjorden, Svalbard
FN396778.1, Marine surface sediment, 50°C incubation - Smeerenburgfjorden, Svalbard
ASV147, *Caloranaerobacter*
ASV516, *Caloranaerobacter*
ASV615, *Caloranaerobacter*
AJ431243, *Alvinella pompejana* white tubes - East Pacific Rise
AJ320233, Caminicella sporogenes, Deep sea hydrothermal vent - East Pacific Rise
AJ431244, *Alvinella pompejana* white tubes - East Pacific Rise
AJ431245, *Alvinella pompejana* white tubes - East Pacific Rise
AJ874301, Hydrothermal black chimney, 60°C enrichment culture - Rainbow field, Mid-Atlantic Ridge
AJ874305, Hydrothermal black chimney, 60°C enrichment culture - Rainbow field, Mid-Atlantic Ridge
AJ874310, Hydrothermal black chimney, 60°C enrichment culture - Rainbow field, Mid-Atlantic Ridge
AJ874312, Hydrothermal black chimney, 60°C enrichment culture - Rainbow field, Mid-Atlantic Ridge
ASV43, *Caminicella*
KX956036.1, Water column and sediment - Aarhus Bay, Denmark
MN463066.1, Marine sediment
JN539926.1, Hypersaline microbial mat, Guerrero Negro - Baja California Sur, Mexico
JN538308.1, Hypersaline microbial mat, Guerrero Negro - Baja California Sur, Mexico
JN539026.1, Hypersaline microbial mat, Guerrero Negro - Baja California Sur, Mexico
FN667354, Compost - Lahti, Finland
FN396772, Marine surface sediment, 50°C incubation - Smeerenburgfjorden, Svalbard
KM823684, River sediment - China
JQ407283, Mud volcano, Lei-gong-huo - eastern Taiwan
HQ916619, Mud volcano, Lei-gong-huo - eastern Taiwan
HQ916607, Mud volcano, Lei-gong-huo - eastern Taiwan
KF758687, Deep sea water
KF964589, Wetland soil - Ebinur lake
JN539026, Hypersaline mat, Guerrero Negro - Baja California Sur, Mexico
JN537682, Hypersaline mat, Guerrero Negro - Baja California Sur, Mexico
JQ407274, Mud volcano, Lei-gong-huo - eastern Taiwan
FN356285, Produced water, 80°C in situ oil reservoir temperature - Dan and Halfdan oil fields, North Sea
FN356288, Produced water, 80°C in situ oil reservoir temperature - Dan and Halfdan oil fields, North Sea
FN356295, Produced water, 80°C in situ oil reservoir temperature - Dan and Halfdan oil fields, North Sea
DQ647144, Produced water, 70°C in situ oil field temperature - Troll Formation, North Sea
FN356335, Produced water, 80°C in situ oil reservoir temperature - Dan and Halfdan oil fields, North Sea
FN356327, Produced water, 80°C in situ oil reservoir temperature - Dan and Halfdan oil fields, North Sea
FN356332, Produced water, 80°C in situ oil reservoir temperature - Dan and Halfdan oil fields, North Sea
FN356342, Produced water, 80°C in situ oil reservoir temperature - Dan and Halfdan oil fields, North Sea
FN356328, Produced water, 80°C in situ oil reservoir temperature - Dan and Halfdan oil fields, North Sea
FN356302, Produced water, 80°C in situ oil reservoir temperature - Dan and Halfdan oil fields, North Sea
FN356340, Produced water, 80°C in situ oil reservoir temperature - Dan and Halfdan oil fields, North Sea
FN356237, Produced water, 80°C in situ oil reservoir temperature - Dan and Halfdan oil fields, North Sea
FN356323, Produced water, 80°C in situ oil reservoir temperature - Dan and Halfdan oil fields, North Sea
DQ647125, Produced water, 70°C in situ oil field temperature - Troll Formation, North Sea
FN356239, Produced water, 80°C in situ oil reservoir temperature - Dan and Halfdan oil fields, North Sea
FN356341, Produced water, 80°C in situ oil reservoir temperature - Dan and Halfdan oil fields, North Sea
FN356304, Produced water, 80°C in situ oil reservoir temperature - Dan and Halfdan oil fields, North Sea
FN356314, Produced water, 80°C in situ oil reservoir temperature - Dan and Halfdan oil fields, North Sea
FN356303, Produced water, 80°C in situ oil reservoir temperature - Dan and Halfdan oil fields, North Sea
X77837
GU118213, Coral - Caribbean
KC668910, Coral - Red Sea
KC668846.1, Coral - Red Sea
KC668846, Coral - Red Sea
KC668837, Coral - Red Sea
KP305708.1, Reef coral - Luhuitou fringing reef, China
HQ606285.1, Marine sediments - South China Sea
KT973497.1, Intertidal outcrops - Isla de Mona, Puerto Rico
GQ267134.1, Hydrothermal sediments - Mothra Field, Juan de Fuca Ridge
HQ696463.1, Deep sea sediment - Indian Ocean
ASV41, *Paramaledivibacter*
FR695371.1, Marine sediment, 25°C incubation - Aarhus Bay, Denmark
DQ831102.1
ASV2045, *Paramaledivibacter*
ASV60, *Paramaledivibacter*
KX062021, Hot spring, Polichnitos - Lesvos, Greece
AF458779, *Paramaledivibacter caminithermalis*, Deep sea hydrothermal chimney - Atlantic Ocean Ridge
FJ203551.1, Coral - Caribbean
ASV165, *Paramaledivibacter*
KC668883.1, Coral - Red Sea
KC668869.1, Coral - Red Sea
KC668910.1, Coral - Red Sea
EU573106, Produced water, 131°C in situ oil reservoir temperature - Ekofisk oil field, North Sea
HQ696463, Deep sea sediment - Indian Ocean
AB806232, Ocean drilling core - Shimokita Peninsula, Japan
FJ203551, Coral - Caribbean
FJ202390, Coral - Caribbean
JQ515752, Coral - Caribbean
KC631808, Hypersaline microbial mat - Kiribati
EF123532, Coral - Caribbean
DQ446118, Coral - Caribbean
JX391232, Surface marine sediment - Hong Kong, China
KC668891, Coral - Red Sea
KT783480, Wukongibacter baidiensis, Deep sea hydrothermal field - Southwest Indian Ridge
JMSU01000863, Marine intertidal flat - Wadden Sea, Germany
AB806231, Ocean drilling core - Shimokita Peninsula, Japan

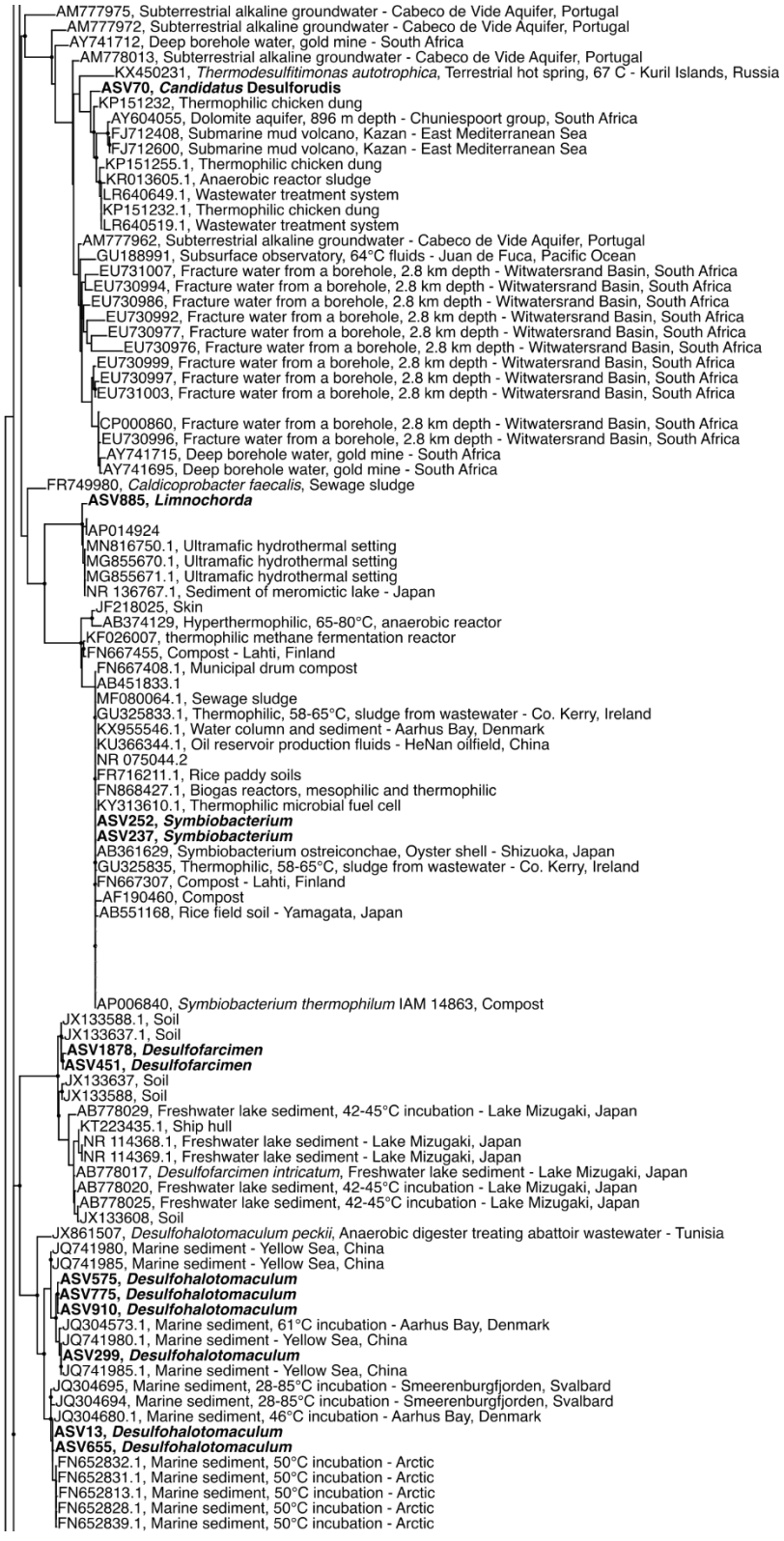
AM777975, Subterrestrial alkaline groundwater - Cabeco de Vide Aquifer, Portugal
AM777972, Subterrestrial alkaline groundwater - Cabeco de Vide Aquifer, Portugal
AY741712, Deep borehole water, gold mine - South Africa
AM778013, Subterrestrial alkaline groundwater - Cabeco de Vide Aquifer, Portugal
KX450231, Thermodesulfitimonas autotrophica, Terrestrial hot spring, 67 C - Kuril Islands, Russia
ASV70, Candidatus Desulforudis
KP151232, Thermophilic chicken dung
AY604055, Dolomite aquifer, 896 m depth - Chuniespoort group, South Africa
FJ712408, Submarine mud volcano, Kazan - East Mediterranean Sea
FJ712600, Submarine mud volcano, Kazan - East Mediterranean Sea
KP151255.1, Thermophilic chicken dung
KR013605.1, Anaerobic reactor sludge
LR640649.1, Wastewater treatment system
KP151232.1, Thermophilic chicken dung
LR640519.1, Wastewater treatment system
AM777962, Subterrestrial alkaline groundwater - Cabeco de Vide Aquifer, Portugal
GU188991, Subsurface observatory, 64°C fluids - Juan de Fuca, Pacific Ocean
EU731007, Fracture water from a borehole, 2.8 km depth - Witwatersrand Basin, South Africa
EU730994, Fracture water from a borehole, 2.8 km depth - Witwatersrand Basin, South Africa
EU730986, Fracture water from a borehole, 2.8 km depth - Witwatersrand Basin, South Africa
EU730992, Fracture water from a borehole, 2.8 km depth - Witwatersrand Basin, South Africa
EU730977, Fracture water from a borehole, 2.8 km depth - Witwatersrand Basin, South Africa
EU730976, Fracture water from a borehole, 2.8 km depth - Witwatersrand Basin, South Africa
EU730999, Fracture water from a borehole, 2.8 km depth - Witwatersrand Basin, South Africa
EU730997, Fracture water from a borehole, 2.8 km depth - Witwatersrand Basin, South Africa
EU731003, Fracture water from a borehole, 2.8 km depth - Witwatersrand Basin, South Africa
CP000860, Fracture water from a borehole, 2.8 km depth - Witwatersrand Basin, South Africa
EU730996, Fracture water from a borehole, 2.8 km depth - Witwatersrand Basin, South Africa
AY741715, Deep borehole water, gold mine - South Africa
AY741695, Deep borehole water, gold mine - South Africa
FR749980, Caldicoprobacter faecalis, Sewage sludge
ASV885, Limnochorda
AP014924
MN816750.1, Ultramafic hydrothermal setting
MG855670.1, Ultramafic hydrothermal setting
MG855671.1, Ultramafic hydrothermal setting
NR 136767.1, Sediment of meromictic lake - Japan
JF218025, Skin
AB374129, Hyperthermophilic, 65-80°C, anaerobic reactor
KF026007, thermophilic methane fermentation reactor
FN667455, Compost - Lahti, Finland
FN667408.1, Municipal drum compost
AB451833.1
MF080064.1, Sewage sludge
GU325833.1, Thermophilic, 58-65°C, sludge from wastewater - Co. Kerry, Ireland
KX955546.1, Water column and sediment - Aarhus Bay, Denmark
KU366344.1, Oil reservoir production fluids - HeNan oilfield, China
NR 075044.2
FR716211.1, Rice paddy soils
FN868427.1, Biogas reactors, mesophilic and thermophilic
KY313610.1, Thermophilic microbial fuel cell
ASV252, Symbiobacterium
ASV237, Symbiobacterium
AB361629, Symbiobacterium ostreiconchae, Oyster shell - Shizuoka, Japan
GU325835, Thermophilic, 58-65°C, sludge from wastewater - Co. Kerry, Ireland
FN667307, Compost - Lahti, Finland
AF190460, Compost
AB551168, Rice field soil - Yamagata, Japan
AP006840, Symbiobacterium thermophilum IAM 14863, Compost
JX133588.1, Soil
JX133637.1, Soil
ASV1878, Desulfofarcimen
ASV451, Desulfofarcimen
JX133637, Soil
JX133588, Soil
AB778029, Freshwater lake sediment, 42-45°C incubation - Lake Mizugaki, Japan
KT223435.1, Ship hull
NR 114368.1, Freshwater lake sediment - Lake Mizugaki, Japan
NR 114369.1, Freshwater lake sediment - Lake Mizugaki, Japan
AB778017, Desulfofarcimen intricatum, Freshwater lake sediment - Lake Mizugaki, Japan
AB778020, Freshwater lake sediment, 42-45°C incubation - Lake Mizugaki, Japan
AB778025, Freshwater lake sediment, 42-45°C incubation - Lake Mizugaki, Japan
JX133608, Soil
JX861507, Desulfohalotomaculum peckii, Anaerobic digester treating abattoir wastewater - Tunisia
JQ741980, Marine sediment - Yellow Sea, China
JQ741985, Marine sediment - Yellow Sea, China
ASV575, Desulfohalotomaculum
ASV775, Desulfohalotomaculum
ASV910, Desulfohalotomaculum
JQ304573.1, Marine sediment, 61°C incubation - Aarhus Bay, Denmark
JQ741980.1, Marine sediment - Yellow Sea, China
ASV299, Desulfohalotomaculum
JQ741985.1, Marine sediment - Yellow Sea, China
JQ304695, Marine sediment, 28-85°C incubation - Smeerenburgfjorden, Svalbard
JQ304694, Marine sediment, 28-85°C incubation - Smeerenburgfjorden, Svalbard
JQ304680.1, Marine sediment, 46°C incubation - Aarhus Bay, Denmark
ASV13, Desulfohalotomaculum
ASV655, Desulfohalotomaculum
FN652832.1, Marine sediment, 50°C incubation - Arctic
FN652831.1, Marine sediment, 50°C incubation - Arctic
FN652813.1, Marine sediment, 50°C incubation - Arctic
FN652828.1, Marine sediment, 50°C incubation - Arctic
FN652839.1, Marine sediment, 50°C incubation - Arctic

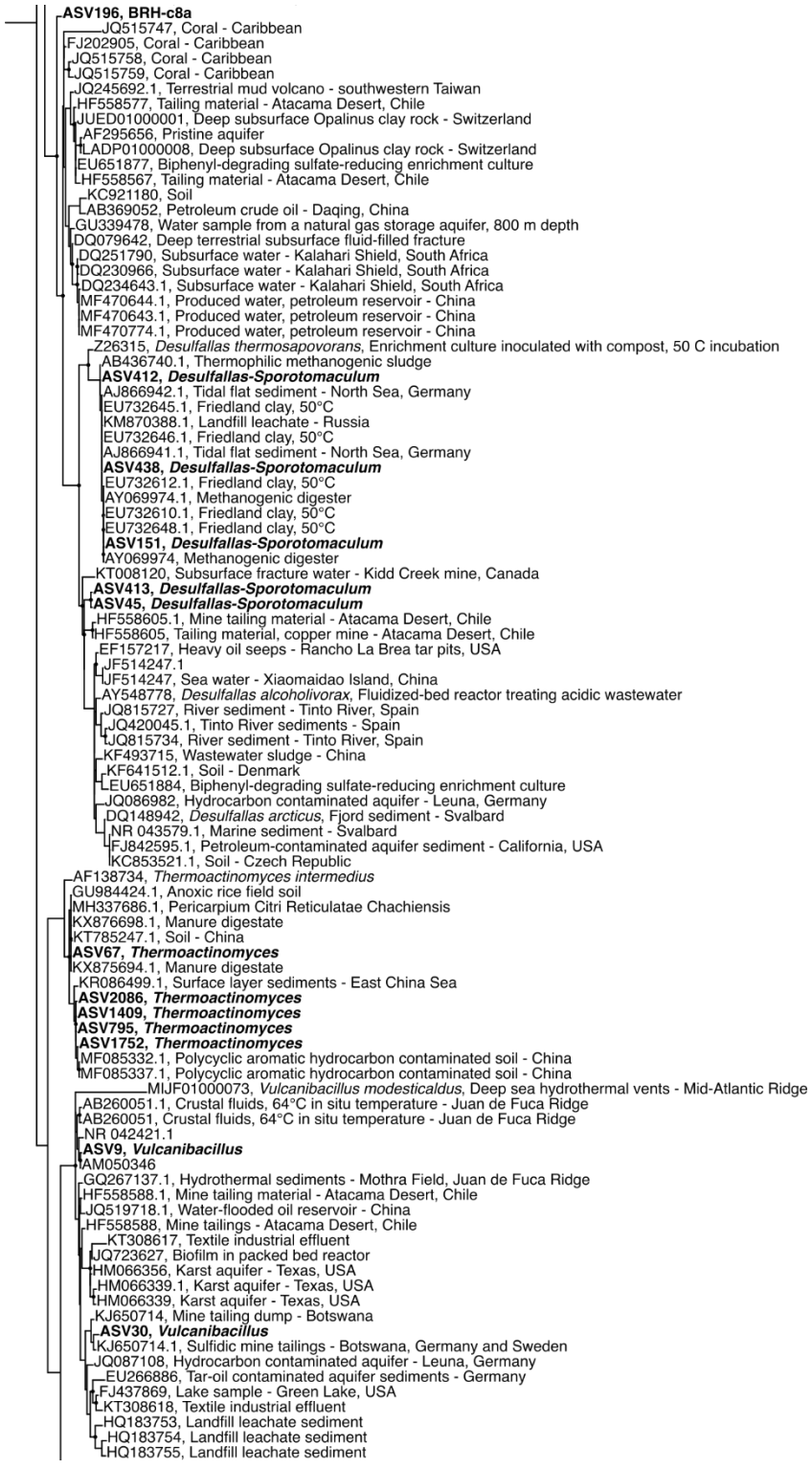
ASV196, BRH-c8a
JQ515747, Coral - Caribbean
FJ202905, Coral - Caribbean
JQ515758, Coral - Caribbean
JQ515759, Coral - Caribbean
JQ245692.1, Terrestrial mud volcano - southwestern Taiwan
HF558577, Tailing material - Atacama Desert, Chile
JUED01000001, Deep subsurface Opalinus clay rock - Switzerland
AF295656, Pristine aquifer
LADP01000008, Deep subsurface Opalinus clay rock - Switzerland
EU651877, Biphenyl-degrading sulfate-reducing enrichment culture
HF558567, Tailing material - Atacama Desert, Chile
KC921180, Soil
AB369052, Petroleum crude oil - Daqing, China
GU339478, Water sample from a natural gas storage aquifer, 800 m depth
DQ079642, Deep terrestrial subsurface fluid-filled fracture
DQ251790, Subsurface water - Kalahari Shield, South Africa
DQ230966, Subsurface water - Kalahari Shield, South Africa
DQ234643.1, Subsurface water - Kalahari Shield, South Africa
MF470644.1, Produced water, petroleum reservoir - China
MF470643.1, Produced water, petroleum reservoir - China
MF470774.1, Produced water, petroleum reservoir - China
Z26315, *Desulfallas thermosapovorans*, Enrichment culture inoculated with compost, 50 C incubation
AB436740.1, Thermophilic methanogenic sludge
ASV412, *Desulfallas-Sporotomaculum*
AJ866942.1, Tidal flat sediment - North Sea, Germany
EU732645.1, Friedland clay, 50°C
KM870388.1, Landfill leachate - Russia
EU732646.1, Friedland clay, 50°C
AJ866941.1, Tidal flat sediment - North Sea, Germany
ASV438, *Desulfallas-Sporotomaculum*
EU732612.1, Friedland clay, 50°C
AY069974.1, Methanogenic digester
EU732610.1, Friedland clay, 50°C
EU732648.1, Friedland clay, 50°C
ASV151, *Desulfallas-Sporotomaculum*
AY069974, Methanogenic digester
KT008120, Subsurface fracture water - Kidd Creek mine, Canada
ASV413, *Desulfallas-Sporotomaculum*
ASV45, *Desulfallas-Sporotomaculum*
HF558605.1, Mine tailing material - Atacama Desert, Chile
HF558605, Tailing material, copper mine - Atacama Desert, Chile
EF157217, Heavy oil seeps - Rancho La Brea tar pits, USA
JF514247.1
JF514247, Sea water - Xiaomaidao Island, China
AY548778, *Desulfallas alcoholivorax*, Fluidized-bed reactor treating acidic wastewater
JQ815727, River sediment - Tinto River, Spain
JQ420045.1, Tinto River sediments - Spain
JQ815734, River sediment - Tinto River, Spain
KF493715, Wastewater sludge - China
KF641512.1, Soil - Denmark
EU651884, Biphenyl-degrading sulfate-reducing enrichment culture
JQ086982, Hydrocarbon contaminated aquifer - Leuna, Germany
DQ148942, *Desulfallas arcticus*, Fjord sediment - Svalbard
NR 043579.1, Marine sediment - Svalbard
FJ842595.1, Petroleum-contaminated aquifer sediment - California, USA
KC853521.1, Soil - Czech Republic
AF138734, *Thermoactinomyces intermedius*
GU984424.1, Anoxic rice field soil
MH337686.1, Pericarpium Citri Reticulatae Chachiensis
KX876698.1, Manure digestate
KT785247.1, Soil - China
ASV67, *Thermoactinomyces*
KX875694.1, Manure digestate
KR086499.1, Surface layer sediments - East China Sea
ASV2086, *Thermoactinomyces*
ASV1409, *Thermoactinomyces*
ASV795, *Thermoactinomyces*
ASV1752, *Thermoactinomyces*
MF085332.1, Polycyclic aromatic hydrocarbon contaminated soil - China
MF085337.1, Polycyclic aromatic hydrocarbon contaminated soil - China
MIJF01000073, *Vulcanibacillus modesticaldus*, Deep sea hydrothermal vents - Mid-Atlantic Ridge
AB260051.1, Crustal fluids, 64°C in situ temperature - Juan de Fuca Ridge
AB260051, Crustal fluids, 64°C in situ temperature - Juan de Fuca Ridge
NR 042421.1
ASV9, *Vulcanibacillus*
AM050346
GQ267137.1, Hydrothermal sediments - Mothra Field, Juan de Fuca Ridge
HF558588.1, Mine tailing material - Atacama Desert, Chile
JQ519718.1, Water-flooded oil reservoir - China
HF558588, Mine tailings - Atacama Desert, Chile
KT308617, Textile industrial effluent
JQ723627, Biofilm in packed bed reactor
HM066356, Karst aquifer - Texas, USA
HM066339.1, Karst aquifer - Texas, USA
HM066339, Karst aquifer - Texas, USA
KJ650714, Mine tailing dump - Botswana
ASV30, *Vulcanibacillus*
KJ650714.1, Sulfidic mine tailings - Botswana, Germany and Sweden
JQ087108, Hydrocarbon contaminated aquifer - Leuna, Germany
EU266886, Tar-oil contaminated aquifer sediments - Germany
FJ437869, Lake sample - Green Lake, USA
KT308618, Textile industrial effluent
HQ183753, Landfill leachate sediment
HQ183754, Landfill leachate sediment
HQ183755, Landfill leachate sediment

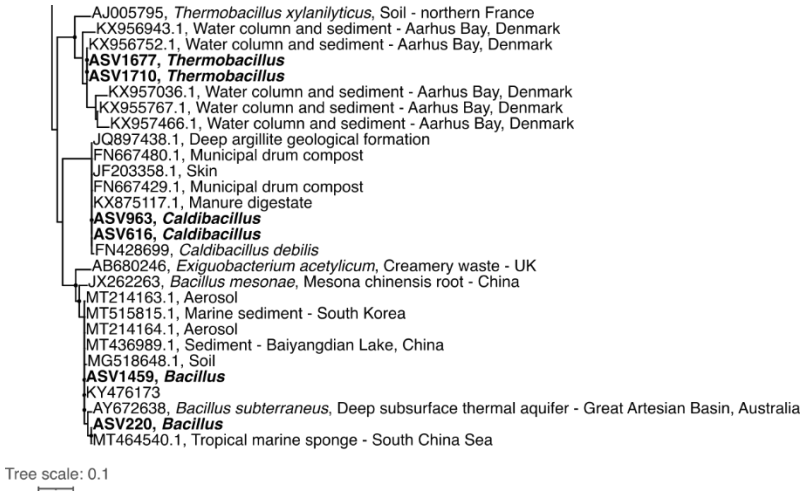

Fig. S4. Phylogenetic association of seep-associated sequences with sequences from other environments. Maximum likelihood tree showing phylogenetic relationships between 42 seep-associated ASVs (bold) and close relatives in the GenBank database. Black circles at the branch nodes indicate >80% bootstrap support (1,000 re-samplings). Scale bar indicates 10% sequence divergence as inferred from PhyML. *Pseudomonas aeruginosa* (accession number Z76672) was used as an outgroup to root the tree.

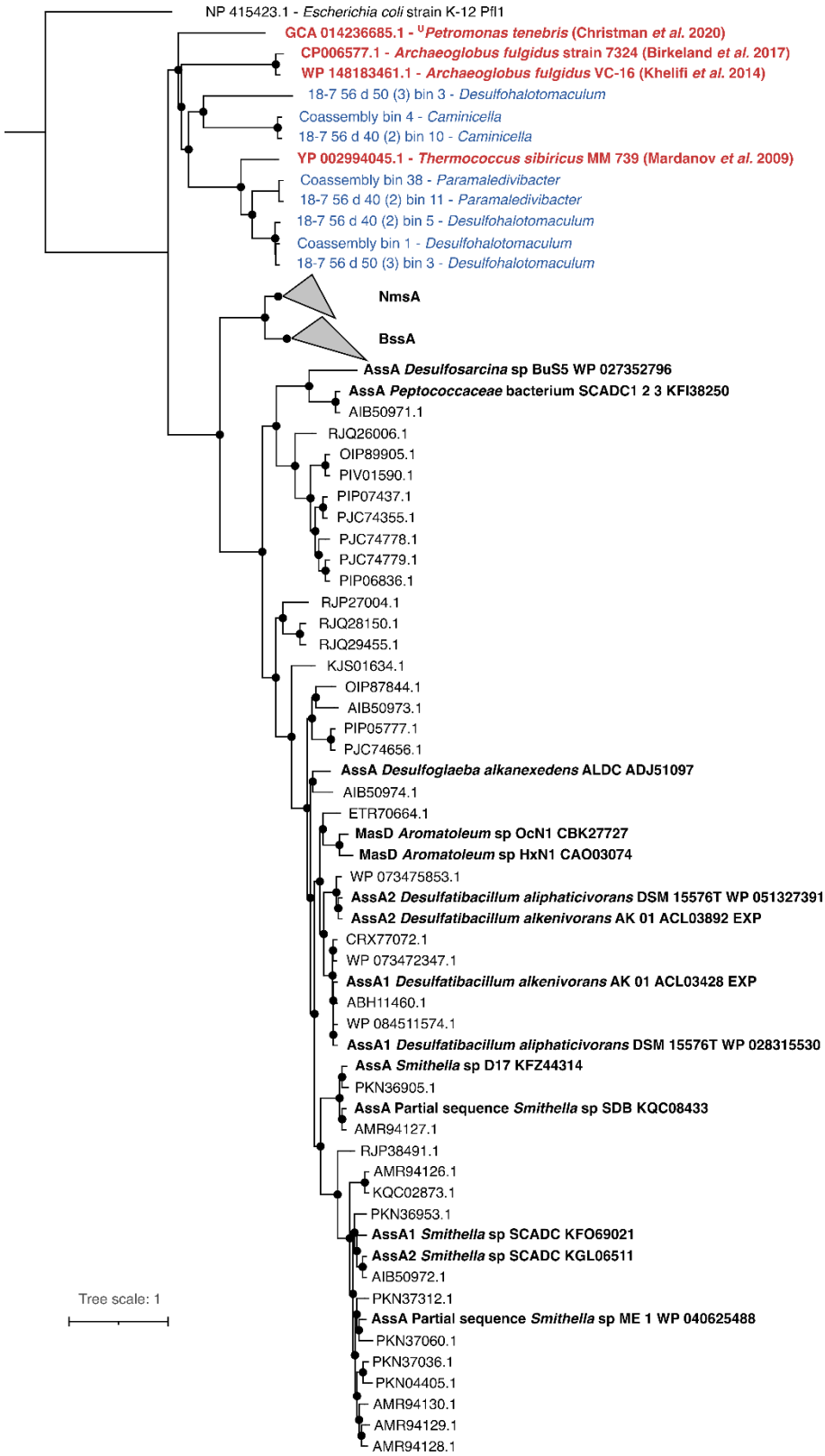
NP 415423.1 - Escherichia coli strain K-12 Pfl1
GCA 014236685.1 - UPetromonas tenebris (Christman et al. 2020)
CP006577.1 - Archaeoglobus fulgidus strain 7324 (Birkeland et al. 2017)
WP 148183461.1 - Archaeoglobus fulgidus VC-16 (Khelifi et al. 2014)
18-7 56 d 50 (3) bin 3 - Desulfohalotomaculum
Coassembly bin 4 - Caminicella
18-7 56 d 40 (2) bin 10 - Caminicella
YP 002994045.1 - Thermococcus sibiricus MM 739 (Mardanov et al. 2009)
Coassembly bin 38 - Paramaledivibacter
18-7 56 d 40 (2) bin 11 - Paramaledivibacter
18-7 56 d 40 (2) bin 5 - Desulfohalotomaculum
Coassembly bin 1 - Desulfohalotomaculum
18-7 56 d 50 (3) bin 3 - Desulfohalotomaculum
NmsA
BssA
AssA Desulfosarcina sp BuS5 WP 027352796
AssA Peptococcaceae bacterium SCADC1 2 3 KFI38250
AIB50971.1
RJQ26006.1
OIP89905.1
PIV01590.1
PIP07437.1
PJC74355.1
PJC74778.1
PJC74779.1
PIP06836.1
RJP27004.1
RJQ28150.1
RJQ29455.1
KJS01634.1
OIP87844.1
AIB50973.1
PIP05777.1
PJC74656.1
AssA Desulfoglaeba alkanexedens ALDC ADJ51097
AIB50974.1
ETR70664.1
MasD Aromatoleum sp OcN1 CBK27727
MasD Aromatoleum sp HxN1 CAO03074
WP 073475853.1
AssA2 Desulfatibacillum aliphaticivorans DSM 15576T WP 051327391
AssA2 Desulfatibacillum alkenivorans AK 01 ACL03892 EXP
CRX77072.1
WP 073472347.1
AssA1 Desulfatibacillum alkenivorans AK 01 ACL03428 EXP
ABH11460.1
WP 084511574.1
AssA1 Desulfatibacillum aliphaticivorans DSM 15576T WP 028315530
AssA Smithella sp D17 KFZ44314
PKN36905.1
AssA Partial sequence Smithella sp SDB KQC08433
AMR94127.1
RJP38491.1
AMR94126.1
KQC02873.1
PKN36953.1
AssA1 Smithella sp SCADC KFO69021
AssA2 Smithella sp SCADC KGL06511
AIB50972.1
PKN37312.1
AssA Partial sequence Smithella sp ME 1 WP 040625488
PKN37060.1
PKN37036.1
PKN04405.1
AMR94130.1
AMR94129.1
AMR94128.1
Tree scale: 1

Fig. S5. Phylogenetic relationships of putative glycyl-radical enzymes with alkylsuccinate synthases. Putative anaerobic alkane-degrading pyruvate-formate lyase enzyme variants from *Desulfohalotomaculum*, *Caminicella* and *Parameldivibacter* thermophilic spores in this study (shown in blue) cluster together with homologous *pflD* gene sequences found in oil reservoir thermophiles [U]*Petromonas tenebris* (*33*), *Archaeoglobus fulgidus* strain 7324 (*37*), and *Thermococcus sibiricus* strain MM 739 (*38*) shown in red. Isolated strains of *Archaeoglobus* and *Thermococcus* have been shown to degrade alkanes in pure culture at high temperature under anaerobic conditions (*86*, *38*). These *pflD* gene sequences, as well as reference sequences of alkane succinate synthase (AssA and MasD) genes also having experimental verification of anaerobic alkane degradation, are shown in bold. Benzyl succinate synthase (BssA) and naphthyl-2-methyl-succinate synthase (NmsA) sequences are represented by collapsed clades. Black circles at the branch nodes indicate >80% bootstrap support (1,000 re-samplings). Scale bar indicates 10% sequence divergence as inferred from PhyML. A sequence of pyruvate formate lyase (Pfl) from *E. coli* was used to root the tree.

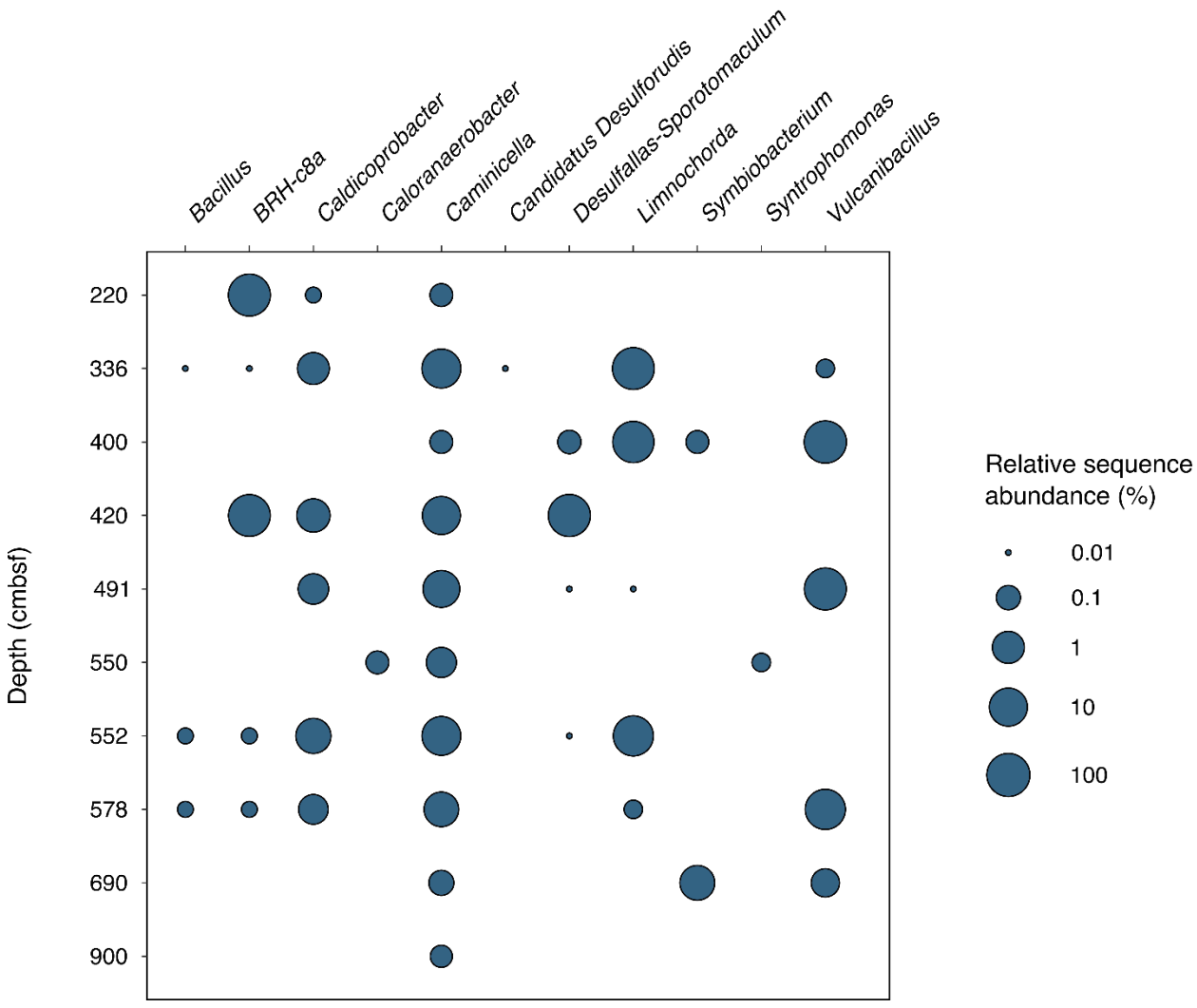

Fig. S6. Endospores remain viable during burial. Detection of endospore-forming bacteria with the same taxonomic classification as seep-associated ASVs (cf. table S5) in deeper Scotian Slope sediment layers following incubation at 50°C. Size of the circles indicates the maximum relative sequence abundance of a taxon in unrarefied sequence libraries at the indicated depth. Based on sediment accumulation rates of 0.1 to 0.2 mm y^{-1} reported in the study area (*45*, *46*), these results confirm spore viability over a 90–180 ka period corresponding to the deepest piston cores (9 mbsf) that were obtained in this study.

Movie S1. Seabed hydrocarbon seepage. Video footage collected using an underwater remotely operated vehicle (ROV) of seabed geofluid flow in the study area (*56*). Vertical hydrocarbon migration rates from a subsurface reservoir to the seabed can be estimated using buoyancy models incorporating Darcy's law (*41*) and estimates on the order of 10 cm d^{-1} reported for seepage of hydrocarbons (*42*).

Table S1. Marine sediment core site locations and sample descriptions. Core number, expedition name, date of core collection, latitude, longitude, water depth, core type and core length.

Table S2. Hydrocarbon geochemical measurements on marine sediment cores. Measurements of interstitial gas composition, interstitial gas isotopes, gas chromatography of the extractable organic matter, and GC-MS of the saturated and aromatic hydrocarbon fractions.

Table S3. ASV table with taxonomic classification of 16S rRNA gene amplicon libraries. Data from 14 core sediments, in triplicate, before incubation (0 d; post-pasteurization) and after 28 (28 d) or 56 (56 d) days of incubation at 40, 50, or 60°C, subsampled to 4,635 sequences.

Table S4. Analysis of similarity (ANOSIM) test results. Microbial community composition differences between subsets of the 16S rRNA gene amplicon libraries for groups of core sediments.

Table S5. IndicSpecies Stat values. Data showing significant associations ($P < 0.05$) of *Firmicutes* ASVs to sediments with geochemical evidence of thermogenic hydrocarbons (n=2) when tested against sediments without geochemical evidence of thermogenic hydrocarbons (n=8) after combined 28 and 56 days of incubation.

Table S6. Taxonomic assignment. Taxonomy (Silva version 138) of 10,860,283 curated 16S rRNA sequences from 59 oil reservoir sequencing surveys.

Table S7. Metagenome-assembled genomes (MAGs). MAG taxonomic classification, completeness (%), contamination (%), genome size (Mbp), GC content, strain heterogeneity, predicted genes and coding density, as well as MAG to amplicon sequence variant (ASV) correlation.

Table S8. Summary of genes detected in metagenome-assembled genomes (MAGs). Genes identified to be required for dissimilatory sulfate reduction, fermentation, hydrocarbon activation, sporulation, glycolysis, and the TCA cycle.

Table S9. Sporulation genes annotated against Pfam, TIGRFAM and Swiss-Prot databases.
Data includes sporulation genes detected in 15 MAGs.

REFERENCES AND NOTES

1. C. Darwin, *On the Origin of Species by Means of Natural Selection, or Preservation of Favoured Races in the Struggle for Life* (J. Murray, 1859).

2. L. G. M. Baas Becking, *Geobiologie of Inleiding Tot de Milieukunde* (W. P. Van Stockum & Zoon, 1934).

3. C. A. Hanson, J. A. Fuhrman, M. C. Horner-Devine, J. B. H. Martiny, Beyond biogeographic patterns: Processes shaping the microbial landscape. *Nat. Rev. Microbiol.* **10**, 497–506 (2012).

4. B. A Ward, B. B. Cael, S. Collins, C. R. Young, Selective constraints on global plankton dispersal. *Proc. Natl. Acad. Sci. U.S.A.* **118**, e2007388118 (2021).

5. B. Setlow, S. Atluri, R. Kitchel, K. Koziol-Dube, P. Setlow, Role of dipicolinic acid in resistance and stability of spores of *Bacillus subtilis* with or without DNA-protective α/β-type small acid-soluble proteins. *J. Bacteriol.* **188**, 3740–3747 (2006).

6. J. S. Fang, C. Kato, G. M. Runko, Y. Nogi, T. Hori, J. T. Li, Y. Morono, F. Inagaki, Predominance of viable spore-forming piezophilic bacteria in high-pressure enrichment cultures from ~1.5 to 2.4 km-deep coal-bearing sediments below the ocean floor. *Front. Microbiol.* **8**, 137 (2017).

7. J. T. Lennon, S. E. Jones, Microbial seed banks: The ecological and evolutionary implications of dormancy. *Nat. Rev. Microbiol.* **9**, 119–130 (2011).

8. M. Mestre, J. Höfer, The microbial conveyor belt: Connecting the globe through dispersion and dormancy. *Trends Microbiol.* **29**, 482–492 (2021).

9. Y. M. Bar-On, R. Phillips, R. Milo, The biomass distribution on Earth. *Proc. Natl. Acad. Sci. U.S.A.* **115**, 6506–6511 (2018).

10. V. B. Heuer, F. Inagaki, Y. Morono, Y. Kubo, A. J. Spivack, B. Viehweger, T. Treude, F. Beulig, F. Schubotz, S. Tonai, S. A. Bowden, M. Cramm, S. Henkel, T. Hirose, K. Homola, T. Hoshino, A. Ijiri, H. Imachi, N. Kamiya, M. Kaneko, L. Lagostina, H. Manners, H. McClelland, K. Metcalfe, N. Okutsu, D. Pan, M. J. Raudsepp, J. Sauvage, M. Tsang, D. T. Wang, E. Whitaker, Y. Yamamoto, K. Yang, L. Maeda, R. R. Adhikari, C. Glombitza, Y. Hamada, J. Kallmeyer, J. Wendt, L. Wörmer, Y. Yamada, M. Kinoshita, K. Hinrichs, Temperature limits to deep subseafloor life in the Nankai Trough subduction zone. *Science* **370**, 1230–1234 (2020).

11. L. Wörmer, T. Hoshino, M. W. Bowles, B. Viehweger, R. R. Adhikari, N. Xiao, G. Uramoto, M. Könneke, C. S. Lazar, Y. Morono, F. Inagaki, K. Hinrichs, Microbial dormancy in the marine subsurface: Global endospore abundance and response to burial. *Sci. Adv.* **5**, eaav1024 (2019).

12. B. A. Lomstein, A. T. Langerhuus, S. D'Hondt, B. B. Jørgensen, A. J. Spivack, Endospore abundance, microbial growth and necromass turnover in deep sub-seafloor sediment. *Nature* **484**, 101–104 (2012).

13. C. R. Hubert, T. B. Oldenburg, M. Fustic, N. D. Gray, S. R. Larter, K. Penn, A. K. Rowan, R. Seshadri, A. Sherry, R. Swainsbury, Massive dominance of *Epsilonproteobacteria* in formation waters from a Canadian oil sands reservoir containing severely biodegraded oil. *Environ. Microbiol.* **14**, 387–404 (2012).

14. V. J. Orphan, L. T. Taylor, D. Hafenbradl, E. F. Delong, Culture-dependent and culture independent characterization of microbial assemblages associated with high-temperature petroleum reservoirs. *Appl. Environ. Microbiol.* **66**, 700–711 (2001).

15. Vigneron, E. B. Alsop, B. P. Lomans, N. C. Kyrpides, I. M. Head, N. Tsesmetzis, Succession in the petroleum reservoir microbiome through an oil field production lifecycle. *ISME J.* **11**, 2141–2154 (2017).

16. B. Bennett, J. J. Adams, N. D. Gray, A. Sherry, T. B. P. Oldenburg, H. Huang, S. R. Larter, I. M. Head, The controls on the composition of biodegraded oils in the deep subsurface—Part 3. The impact of microorganism distribution on petroleum geochemical gradients in biodegraded petroleum reservoirs. *Org. Geochem.* **56**, 94–105 (2013).

17. A. G. Judd, The global importance and context of methane escape from the seabed. *Geo-Mar. Lett.* **23**, 147–154 (2003).

18. A. L. Müller, J. R. de Rezende, C. R. J. Hubert, K. U. Kjeldsen, I. Lagkouvardos, D. Berry, B. B. Jørgensen, A. Loy, Endospores of thermophilic bacteria as tracers of microbial dispersal by ocean currents. *ISME J.* **8**, 1153–1165 (2014).

19. C. A. Hanson, A. L. Müller, A. Loy, C. Dona, R. Appel, B. B. Jørgensen, C. R. J. Hubert, Historical factors associated with past environments influence the biogeography of thermophilic endospores in Arctic marine sediments. *Front. Microbiol.* **10**, 245 (2019).

20. C. Hubert, A. Loy, M. Nickel, C. Arnosti, C. Baranyi, V. Bruchert, T. Ferdelman, K. Finster, F. M. Christensen, J. R. de Rezende, V. Vandieken, B. B. Jørgensen, A constant flux of diverse thermophilic bacteria into the cold Arctic seabed. *Science* **325**, 1541–1544 (2009).

21. I. R. MacDonald, Natural and unnatural oil slicks in the Gulf of Mexico. *J. Geophys. Res. Oceans* **120**, 8364–8380 (2015).

22. A. Chakraborty, E. Ellefson, C. Li, D. Gittins, J. M. Brooks, B. B. Bernard, C. R. J. Hubert, Thermophilic endospores associated with migrated thermogenic hydrocarbons in deep Gulf of Mexico marine sediments. *ISME J.* **12**, 1895–1906 (2018).

23. A. Chakraborty, S. E. Ruff, X. Dong, E. D. Ellefson, C. Li, J. M. Brooks, J. McBee, B. B. Bernard, C. R. J. Hubert, Hydrocarbon seepage in the deep seabed links subsurface and seafloor biospheres. *Proc. Natl. Acad. Sci. U.S.A.* **117**, 11029–11037 (2020).

24. J. Kallmeyer, R. Pockalny, R. R. Adhikari, D. C. Smith, S. D'Hondt, Global distribution of microbial abundance and biomass in subseafloor sediment. *Proc. Natl. Acad. Sci. U.S.A.* **109**, 16213–16216 (2012).

25. M. A. Abrams, Marine seepage variability and its impact on evaluating the surface migrated hydrocarbon seep signal. *Mar. Pet. Geol.* **121**, 104600 (2020).

26. N. C. Nanda, Direct hydrocarbon indicators (DHI), in *Seismic Data Interpretation and Evaluation for Hydrocarbon Exploration and Production*, N. C. Nanda, Ed. (Springer, 2016), pp. 103–113.

27. A. G. Judd, M. Hovland, in *Seabed Fluid Flow: The Impact on Geology, Biology and the Marine Environment* (Cambridge Univ. Press, 2007), pp. 163–178.

28. L. B. Magoon, W. G. Dow, *The Petroleum System—From Source to Trap* (American Association of Petroleum Geologists, 1994).

29. M. Y. Galperin, Genome diversity of spore-forming *Firmicutes*. *Microbiol. Spectr.* **1**, 10.1128/microbiolspectrum.TBS-0015-2012 (2013).

30. J. R. de Rezende, C. R. J. Hubert, H. Røy, K. U. Kjeldsen, B. B. Jørgensen, Estimating the abundance of endospores of sulfate-reducing bacteria in environmental samples by inducing germination and exponential growth. *Geomicrobiol. J.* **34**, 338–345 (2017).

31. T. Wunderlin, T. Junier, L. Roussel-Delif, N. Jeanneret, P. Junier, Endospore-enriched sequencing approach reveals unprecedented diversity of Firmicutes in sediments. *Environ. Microbiol. Rep.* **6**, 631–639 (2014).

32. H. Dahle, F. Garshol, M. Madsen, N. L. Birkeland, Microbial community structure analysis of produced water from a high-temperature North Sea oil-field. *Antonie Van Leeuwenhoek* **93**, 37–49 (2008).

33. G. D. Christman, R. I. León-Zayas, R. Zhao, Z. M. Summers, J. F. Biddle, Novel clostridial lineages recovered from metagenomes of a hot oil reservoir. *Sci. Rep.* **10**, 8048 (2020).

34. D. M. Jones, I. M. Head, N. D. Gray, J. J. Adams, A. K. Rowan, C. M. Aitken, B. Bennett, H. Huang, A. Brown, B. F. J. Bowler, T. Oldenburg, M. Erdmann, S. R. Larter. Crude-oil biodegradation via methanogenesis in subsurface petroleum reservoirs. *Nature* **451**, 176–180 (2008).

35. N. D. Gray, A. Sherry, S. R. Larter, M. Erdmann, J. Leyris, T. Liengen, J. Beeder, I. M. Head, Biogenic methane production in formation waters from a large gas field in the North Sea. *Extremophiles* **13**, 511–519 (2009).

36. V. Khot, J. Zorz, D. A. Gittins, A. Chakraborty, E. Bell, M. A. Bautista, A. J. Paquette, A. K. Hawley, B. Novotnik, C. R. J. Hubert, M. Strous, S. Bhatnagar, CANT-HYD: A curated database of phylogeny-derived Hidden Markov Models for annotation of marker genes involved in hydrocarbon degradation. *Front. Microbiol.* **12**, 764058 (2022).

7. N. K. Birkeland, P. Schönheit, L. Poghosyan, A. Fiebig, H. P. Klenk, Complete genome sequence analysis of *Archaeoglobus fulgidus* strain 7324 (DSM 8774), a hyperthermophilic archaeal sulfate reducer from a North Sea oil field. *Stand Genomic Sci.* **12**, 79 (2017).

38. A. V. Mardanov, N. V. Ravin, V. A. Svetlitchnyi, A. V. Beletsky, M. L. Miroshnichenko, E. A. Bonch-Osmolovskaya, K. G. Skryabin, Metabolic versatility and indigenous origin of the archaeon *Thermococcus sibiricus*, isolated from a Siberian oil reservoir, as revealed by genome analysis. *Appl. Environ. Microbiol.* **75**, 4580–4588 (2009).

39. J. A. Hoch, Regulation of the phosphorelay and the initiation of sporulation in *Bacillus subtilis*. *Annu. Rev. Microbiol.* **47**, 441–465 (1993).

40. M. E. Deptuck, K. L. Kendell, "Atlas of 3D seismic surfaces and thickness maps, central and southwestern Scotian Slope" (Geoscience Open File Report 2020-002MF and Geoscience Open File Report 2020-001MF to 006MF, Canada-Nova Scotia Offshore Petroleum Board, 2020).

41. G. K. Arp, Effusive microseepage: A first approximation model for light hydrocarbon movement in the subsurface. *Assoc. Pet. Geol. Bull.* **8**, 1–17 (1992).

42. G. K. Rice, Vertical migration in theory and in practice. *Interpretation* **10**, SB17–SB26 (2022).

43. C. G. Hannah, J. A. Shore, J. W. Loder, C. E. Naimie, Seasonal circulation on the western and central Scotian Shelf. *J. Phys. Oceanogr.* **31**, 591–615 (2001).

44. J. R. de Rezende, K. U. Kjeldsen, C. R. J. Hubert, K. Finster, A. Loy, B. B. Jørgensen, Dispersal of thermophilic *Desulfotomaculum* endospores into Baltic Sea sediments over thousands of years. *ISME J.* **7**, 72–84 (2013).

45. K. A. Jenner, D. C. Campbell, J. M. Barnett, J. Higgins, A. Normandeau, Piston cores and supporting high-resolution seismic data, CCGS Hudson Expedition 2015018, Scotian Slope, Canada (Open File 8637, Geological Survey of Canada).

46. D. J. W. Piper, K. I. Skene, Latest Pleistocene ice-rafting events on the Scotian Margin (eastern Canada) and their relationship to Heinrich events. *Paleoceanography* **13**, 205–214 (1998).

47. J. W. Lund, L. Bjelm, G. Bloomquist, A. K. Mortensen, Characteristics, development and utilization of geothermal resources—A Nordic perspective. *Episodes* **31**, 140–147 (2008).

48. F. Beulig, F. Schubert, R. R. Adhikari, C. Glombitza, V. B. Heuer, K. U. Hinrichs, K. L. Homola, F. Inagaki, B. B. Jørgensen, J. Kallmeyer, S. J. Krause, Rapid metabolism fosters microbial survival in the deep, hot subseafloor biosphere. *Nat. Commun.* **13**, 312 (2022).

49. Y. Morono, M. Ito, T. Hoshino, T. Terada, T. Hori, M. Ikehara, S. D'Hondt, F. Inagaki, Aerobic microbial life persists in oxic marine sediment as old as 101.5 million years. *Nat. Commun.* **11**, 3626 (2020).

50. A. Wilhelms, S. R. Larter, I. Head, P. Farrimond, R. di-Primio, C. Zwach, Biodegradation of oil in uplifted basins prevented by deep-burial sterilization. *Nature* **411**, 1034–1037 (2001).

51. J. F. Biddle, J. B. Sylvan, W. J. Brazelton, B. J. Tully, K. J. Edwards, C. L. Moyer, J. F. Heidelberg, W. C. Nelson, Prospects for the study of evolution in the deep biosphere. *Front. Microbiol.* **2**, 285 (2012).

52. M. D. Lynch, J. D. Neufeld, Ecology and exploration of the rare biosphere. *Nat. Rev. Microbiol.* **13**, 217–229 (2015).

53. D. C. Campbell, A. W. A. MacDonald, CCGS Hudson Expedition 2015–018 Geological investigation of potential seabed seeps along the Scotian Slope, June 25–July 9, 2015 (Open File 8116, Geological Survey of Canada, 2016).

54. D. C. Campbell, CCGS Hudson Expedition 2016–011, phase 2. Cold seep investigations on the Scotian Slope, offshore Nova Scotia, June 15–July 6, 2016 (Open File 8525, Geological Survey of Canada, 2019).

55. D. C. Campbell, A. Normandeau, CCGS Hudson Expedition 2018–041: High-resolution investigation of deep-water seabed seeps and landslides along the Scotian Slope, offshore Nova Scotia, May 26–June 15, 2018 (Open File 8567, Geological Survey of Canada, 2019).

56. R. Bennett, P.-A. Desiage, Expedition report 21CONDOR: Scotian Slope, August 14–29, 2021 (Open File 8889, Geological Survey of Canada, 2022).

57. M. F. Isaksen, F. Bak, B. B. Jørgensen, Thermophilic sulfate-reducing bacteria in cold marine sediment. *FEMS Microbiol. Ecol.* **14**, 1–8 (1994).

58. A. Klindworth, E. Pruesse, T. Schweer, J. Peplies, C. Quast, M. Horn, F. O. Glöckner, Evaluation of general 16S ribosomal RNA gene PCR primers for classical and next-generation sequencing-based diversity studies. *Nucleic Acids Res.* **41**, e1 (2013).

59. M. Martin, Cutadapt removes adapter sequences from high-throughput sequencing reads. *EMBnet J.* **17**, 10–12 (2011).

60. J. Callahan, P. J. McMurdie, M. J. Rosen, A. W. Han, A. J. A. Johnson, and S. P. Holmes, DADA2: High-resolution sample inference from Illumina amplicon data. *Nat. Methods* **13**, 581–583 (2016).

61. R Core Team, R: A language and environment for statistical computing (R Foundation for Statistical Computing, 2014); www.R-project.org/.

62. C. Quast, E. Pruesse, P. Yilmaz, J. Gerken, T. Schweer, P. Yarza, J. Peplies, F. O. Glöckner, The SILVA ribosomal RNA gene database project: Improved data processing and web-based tools. *Nucleic Acids Res.* **41**, 590–596 (2013).

63. P. J. McMurdie, S. Holmes, Phyloseq: An R package for reproducible interactive analysis and graphics of microbiome census data. *PLOS ONE* **8**, e61217 (2013).

64. D. Li, C.-M. Liu, R. Luo, K. Sadakane, T.-W. Lam, MEGAHIT: An ultra-fast single-node solution for large and complex metagenomics assembly via succinct de Bruijn graph. *Bioinformatics* **31**, 1674–1676 (2015).

65. D. D. Kang, F. Li, E. Kirton, A. Thomas, R. Egan, H. An, Z. Wang, MetaBAT 2: An adaptive binning algorithm for robust and efficient genome reconstruction from metagenome assemblies. *PeerJ.* **7**, e7359 (2019).

66. D. H. Parks, M. Imelfort, C. T. Skennerton, P. Hugenholtz, G. W. Tyson, CheckM: Assessing the quality of microbial genomes recovered from isolates, single cells, and metagenomes. *Genome Res.* **25**, 1043–1055 (2015).

67. H. R. Gruber-Vodicka, B. K. B. Seah, E. Pruesse, phyloFlash: Rapid small-subunit rRNA profiling and targeted assembly from metagenomes. *mSystems* **5**, e00920-20 (2020).

68. X. Dong, M. Strous, An integrated pipeline for annotation and visualization of metagenomic contigs. *Front. Genet.* **10**, 999 (2019).

69. E. D. Graham, J. F. Heidelberg, B. J. Tully, Potential for primary productivity in a globally-distributed bacterial phototroph. *ISME J.* **350**, 1–6 (2018).

70. M. Kanehisa, Y. Sato, K. Morishima, BlastKOALA and GhostKOALA: KEGG tools for functional characterization of genome and metagenome sequences. *J. Mol. Biol.* **428**, 726–731 (2016).

71. D. Hyatt, G.-L. Chen, P. F. LoCascio, M. L. Land, F. W. Larimer, L. J. Hauser, Prodigal: Prokaryotic gene recognition and translation initiation site identification. *BMC Bioinformatics* **11**, 119 (2010).

72. P. A. Chaumeil, A. J. Mussig, P. Hugenholtz, D. H. Parks, GTDB-Tk: A toolkit to classify genomes with the genome taxonomy database. *Bioinformatics* **36**, 1925–1927 (2019).

73. P. D. Schloss, S. L. Westcott, T. Ryabin, J. R. Hall, M. Hartmann, E. B. Hollister, R. A. Lesniewski, B. B. Oakley, D. H. Parks, C. J. Robinson, J. W. Sahl, B. Stres, G. G. Thallinger, D. J. Van Horn, C. F. Weber, Introducing mothur: Open-source, platform-independent, community-supported software for describing and comparing microbial communities. *Appl. Environ. Microbiol.* **75**, 7537–7541 (2009).

74. M. R. Olm, C. T. Brown, B. Brooks, J. F. Banfield, dRep: A tool for fast and accurate genomic comparisons that enables improved genome recovery from metagenomes through de-replication. *ISME J.* **11**, 2864–2868 (2017).

75. R. Leinonen, H. Sugawara, M. Shumway, The sequence read archive. *Nucleic Acids Res.* **39**, D19–D21 (2011).

76. T. Rognes, T. Flouri, B. Nichols, C. Quince, F. Mahé, VSEARCH: A versatile open source tool for metagenomics. *PeerJ* **4**, e2584 (2016).

77. J. Oksanen, R. Kindt, P. Legendre, B. O'Hara, *The Vegan Package—Community Ecology Package. R package version 2.0–9* (2007).

78. H. Wickham, *ggplot2: Elegant Graphics for Data Analysis* (Springer, ed. 3, 2009).

79. M. De Cáceres, P. Legendre, M. Moretti, Improving indicator species analysis by combining groups of sites. *Oikos* **119**, 1674–1684 (2010).

80. E. Pruesse, J. Peplies, F. O. Glöckner, SINA: Accurate high-throughput multiple sequence alignment of ribosomal RNA genes. *Bioinformatics* **28**, 1823–1829 (2012).

81. W. Ludwig, O. Strunk, R. Westram, L. Richter, H. Meier, Yadhukumar, A. Buchner, T. Lai, S. Steppi, G. Jobb, W. Förster, I. Brettske, S. Gerber, A. W Ginhart, O. Gross, S. Grumann, S. Hermann, R. Jost, A. König, T. Liss, R. Lüssmann, M. May, B. Nonhoff, B. Reichel, R. Strehlow, A. Stamatakis, N. Stuckmann, A. Vilbig, M. Lenke, T. Ludwig, A. Bode, K. Schleifer, ARB: A software environment for sequence data. *Nucleic Acids Res.* **32**, 1363–1371 (2004).

82. I. Letunic, P. Bork, Interactive tree of life (iTOL) v4: Recent updates and new developments. *Nucleic Acids Res.* **47**, W256–W259 (2019).

83. B. A. Lomstein, B. B. Jørgensen, Pre-column liquid chromatographic determination of dipicolinic acid from bacterial endospores. *Limnol. Oceanogr. Methods* **10**, 227–233 (2012).

84. J. E. Rattray, A. Chakraborty, C. Li, G. Elizondo, N. John, M. Wong, J. R. Radović, T. B. P. Oldenburg, C. R. J. Hubert, Sensitive quantification of dipicolinic acid from bacterial endospores in soils and sediments. *Environ. Microbiol.* **23**, 1397–1406 (2021).

85. J. Fichtel, J. Köster, J. Rullkötter, H. Sass, Spore dipicolinic acid contents used for estimating the number of endospores in sediments. *FEMS Microbiol. Ecol.* **61**, 522–532 (2007).

6. N. Khelifi, O. A. Ali, P. Roche, V. Grossi, C. Brochier-Armanet, O. Valette, B. Ollivier, A. Dolla, A. Hirschler-Réa, Anaerobic oxidation of long-chain *n*-alkanes by the hyperthermophilic sulfate-reducing archaeon, *Archaeoglobus fulgidus*. *ISME J.* **8**, 2153–2166 (2014).